EUROPHYSICS LETTERS 1 February 2004

Europhys. Lett., **65** (3), pp. 323–329 (2004)
DOI: 10.1209/epl/i2003-10099-9

Popliteal rippling of layered elastic tubes and scrolls

L. Mahadevan[1](*), J. Bico[2] and G. McKinley[2]

[1] *Department of Applied Mathematics and Theoretical Physics*
University of Cambridge - Wilberforce Road, Cambridge, CB3 0WA, UK
[2] *Department of Mechanical Engineering, Massachusetts Institute of Technology*
77 Mass. Ave., Cambridge, MA 02139, USA

(received 3 September 2003; accepted in final form 26 November 2003)

PACS. 46.32.+x – Static buckling and instability.
PACS. 81.07.De – Nanotubes.
PACS. 47.54.+r – Pattern selection; pattern formation.

Abstract. – Motivated by the periodic ripples observed in bent multi-walled nanotubes, we use macroscopic ideas to derive geometric scaling laws for the wavelength and amplitude of ripples in elastic scrolls and multi-walled tubes. Remarkably, our predictions are essentially independent of material properties, and thus have a range of validity varying from the atomic to the macroscopic even for relatively large deformations. We verify this using experimental data that vary over six orders of magnitude in length, ranging from millimeters to nanometers obtained using materials as disparate as rubber and graphite.

The mechanical response of a slender strut or a tube is very different from the bulk response of the same material, owing primarily to the geometric separation of scales inherent in the structure. This makes the structure relatively flexible and capable of large elastic deformations, a fact that is at the heart of many new material systems. The scale of these soft modes of deformation, such as bending and twisting, is typically determined by a combination of material and geometric properties and gives rise to all manner of instabilities classified under the general rubric of buckling. Understanding the response of the structures beyond the onset of these instabilities is typically made difficult by the combination of geometric and material nonlinearities. However, for small structures as well for those made of soft materials, a reasonable description of the large-deformation behavior requires a consideration of just the geometric nonlinearities, thus making the problem more tractable. In this letter, we treat a class of such systems motivated by the nonlinear mechanical response of layered tubular structures, and show that our geometric scaling laws are consistent with experimental data gathered from phenomena separated by six orders of magnitude in scale.

In fig. 1(a), we see the rippling instability of a bent multi-walled carbon nanotube, where the finite-amplitude periodic ripples have a wavelength that is much larger than the thickness of a single layer, itself a fraction of a nanometer. These deformations are not unique to the nano-world; when a rubber macrotube made by rolling a thin sheet of rubber into a scroll

(*) Current address: Divison of Engineering and Applied Sciences, Harvard University - Cambridge, MA 02138, USA. E-mail: lm@deas.harvard.edu

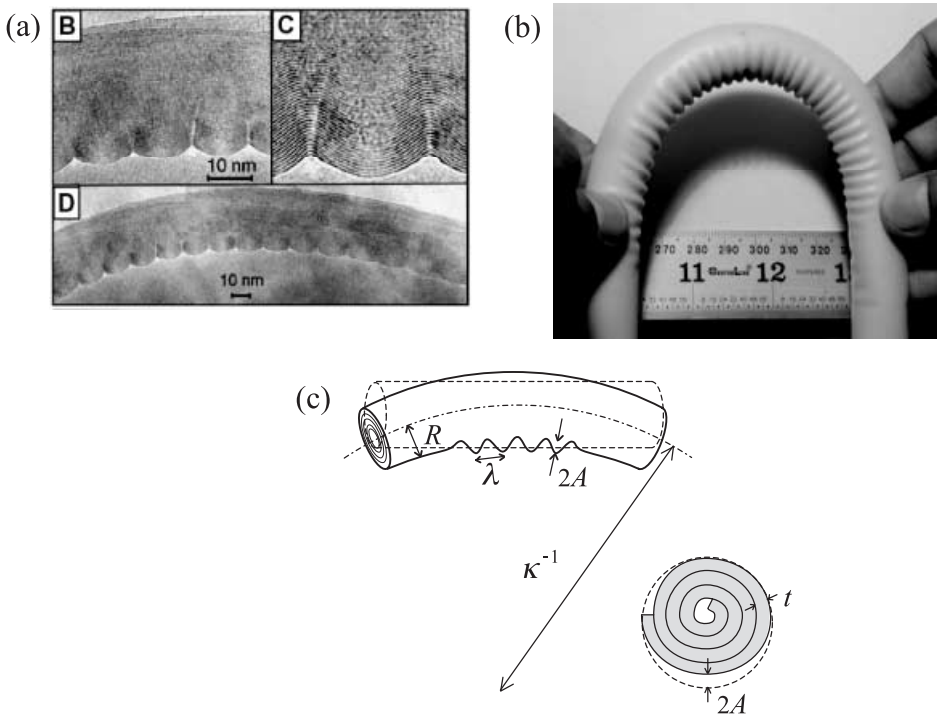

Fig. 1 – The geometric similarities in the rippling of a bent (a) multi-walled carbon nanotube (from [1]) and (b) rubber macrotube suggest that a single theory can explain both. (c) A schematic of the ripples showing our notation.

is bent (fig. 1(b)), we see a similar rippling instability. However, there are two putative qualitative differences between the systems due to this large disparity in scale that we must address first: the effect of thermal fluctuations and the role of short-range forces, both of which could be important for nanotubes. The persistence length of single-wall nanotubes is of the order of meters, and that for multi-walled tubes is even larger, so that thermal effects can be safely neglected in an equilibrium theory. As for the role of short-range forces, their dominant effect is to prevent the inter-penetration of the layers. In the macrotubes, the presence of layers serves the same purpose. Therefore, a single theory can possibly explain both despite the very large disparity in length scales which separate the two phenomena. This hope is bolstered by the fact that experiments on nanotubes [1] and rubber tubes show that the rippling is completely reversible and elastic. In this letter we show that a simple elastic theory that assumes that the strains are small so that the material response is linear and isotropic in each layer [2] but accounts for geometrical nonlinearities suffices to explain these observations quantitatively.

We first give a physical argument for the formation of the popliteal (ham of the knee) ripples in multi-walled tubes. If a long single-walled tube of length L, circular cross-section with external radius R and thickness $t \ll R < L$ is bent into an arc of a circle with curvature κ, the cross-section first ovalizes into the Brazier mode [3]. When the curvature exceeds a critical value, the tube collapses about a knee formed by a sharp ridge connecting two kinks, just like a bent drinking straw [4, 5]. This phenomenon reflects the very large energetic cost of stretching a thin sheet compared to bending it [6]; the ridge allows the shell to respond

by bending almost everywhere except in a small region in the neighborhood of the kinks and the ridge, where large localized deformations arise. In a multi-walled tube, the single sharp ridge is replaced by gentle periodic undulations in the popliteal region. Because the layers are relatively free to slide over each other in the rubber scrolls and multi-walled nanotubes, the steric effect due to the inner walls prevents the Brazier mode of buckling which favors long-wavelength deformations. Instead, the layers are forced to accommodate the geometrically imposed compressive strain due to tube bending by rippling with a relatively short wavelength; this is particularly true when the number of walls is large, and the small hollow core has a negligible effect. The competition between single-layer bending, which favors long-wavelength deformations, and the elastic foundation provided by the multiple layers, which favors short-wavelength deformation, leads to the selection of an intermediate scale of rippling, just as in beam buckling on an elastic foundation [6] or in the wrinkling of skin [7].

We now quantify this physical argument using the schematic in fig. 1(c). If a ripple of wavelength λ leads to a radial displacement of the outer wall of the tube with amplitude A, the typical curvature of the ripple scales as A/λ^2. Note that here we have assumed that the curvature of the ripples is much larger than that of the bent tube, so that we can neglect the fact that A/λ^2 is really the excess curvature over and above that induced by the bending of the tube [8]. Then we may write the elastic bending energy density per layer per unit area as

$$U_{\mathrm{B}} \sim Et^3\kappa^2 \sim Et^3A^2/\lambda^4, \tag{1}$$

where E is Young's modulus of the material and the bending stiffness of a single layer scales as Et^3 [6]. Because the tube walls are curved, the small-scale radial rippling also causes circumferential stretching of the layers in the popliteal region to accommodate the compressive strain induced by the macroscopic bending of the tube. This stretching strain is of order A/R and varies linearly away from the neutral axis of bending. Then the stretching strain energy density per layer (per unit area) is

$$U_{\mathrm{S}} \sim EtA^2/R^2. \tag{2}$$

Although the rippling causes the layers to stretch in the circumferential direction, in the axial direction the layers bend approximately inextensibly. This is a consequence of the high energetic cost of stretching; the layers will always respond inextensibly as long as the geometric constraints and boundary conditions allow it. The initial circumferential curvature of the tube $1/R$ leads to layer stretching when ripples are formed since the ripples change the local radius of the tube; here the constraints prohibit inextensional deformations. However, in the axial direction, there is no initial curvature, so that bending can be and is accomplished approximately inextensibly. For a single ripple on the outer layer, the externally imposed curvature κ leads to a compressive strain of order $R\kappa$. Since this is accommodated by bending the layer out of the plane, the axial inextensibility condition written in terms of Pythagoras' theorem for a single wave yields $[\lambda(1 - R\kappa)]^2 + A^2 \approx \lambda^2$, which simplifies to

$$A^2/\lambda^2 \approx R\kappa. \tag{3}$$

This constraint makes our theory nonlinear from the outset because the amplitude and wavelength of the ripples are related to each other. Substituting (3) into the expressions above for U_{B} and U_{S}, we can write the total energy density as

$$U = U_{\mathrm{B}} + U_{\mathrm{S}} \sim EtR\kappa\left(\frac{t^2}{\lambda^2} + \frac{\lambda^2}{R^2}\right). \tag{4}$$

Integrating the energy in (4) over the (constant) area of a layer, and minimizing U with respect to λ, leads to a scaling law for the wavelength

$$\lambda \sim (Rt)^{1/2}. \tag{5}$$

Using (5) in the inextensibility constraint (3) leads to a scaling law for the maximum ripple amplitude

$$A \sim R(t\kappa)^{1/2}. \tag{6}$$

We observe that the wavelength is essentially independent of the material properties [9] and is also independent of the applied strain/loading. On the other hand, the amplitude is independent of the material properties but is dependent on the externally induced curvature κ. Our scaling laws fall within the scope of a recent general theory of wrinkling [7] with one crucial difference; the layered cylindrical geometry here leads to the surprising independence of the wavelength on all but the system geometry.

We now sketch the main steps of a slightly more involved analysis that allows us to obtain the prefactors for the above scaling laws. In terms of cylindrical polar coordinates (r, θ, x), the radial displacement of the ripples in a single layer is $u(r, \theta, x)$, the curvature due to rippling is $\kappa_r = \partial^2 u/\partial x^2$, while the circumferential stretching strain is $\gamma_r = u/r$. These strains yield the dominant contributions [10] to the total energy density due to bending and stretching in a sheet of thickness t, modulus E and Poisson ratio ν and lead to [6]

$$U = U_{\mathrm{B}} + U_{\mathrm{S}} \approx \frac{Et^3}{24(1-\nu^2)}\kappa_r^2 + \frac{1}{2}Et\gamma_r^2. \tag{7}$$

Since the ripples form as a consequence of the macroscopically imposed curvature of the tube κ, the constraint of axial inextensibility for a layer in the popliteal region reads

$$L = \int_0^{2\pi/k} \left[\frac{1}{2}\left(\frac{\partial u}{\partial x}\right)^2 - \Delta(\kappa)\right] \mathrm{d}x = 0, \tag{8}$$

where $k = 2\pi/\lambda$ is the wave number of the ripples, and $\Delta(\kappa) \approx r\kappa \sin\theta$. Then, the wavelength and amplitude of the ripples are given by minimizing the functional $\int (U_{\mathrm{B}} + U_{\mathrm{S}}) \mathrm{d}a - \Lambda L$, where Λ is a Lagrange multiplier that imposes the inextensibility constraint (8). To be consistent with bending of the tube, the solution of the (linear) Euler-Lagrange equation must have the form $u(r, \theta, x) = A \sin kx \sin\theta$, $\theta \in [0, \pi]$ in the popliteal region, with the amplitude A and wave number k related via the inextensibility constraint (8). Plugging in this form for $u(r, \theta, x)$ into the energy density in (7), integrating over the layer area and minimizing with respect to k yields

$$k^2 = \frac{\left[12(1-\nu^2)\right]^{1/2}}{tr}. \tag{9}$$

For rubber, $\nu \approx 0.5$, so that the wavelength of the ripples on the outer layer where $r = R$ is

$$\lambda = \frac{2\pi}{\sqrt{3}}(tR)^{1/2} \approx 3.6(tR)^{1/2}. \tag{10}$$

The amplitude is determined by satisfying the axial inextensibility constraint in an integrated sense [11], and yields

$$A \approx \frac{2}{\pi^{3/2}}\lambda(\kappa R)^{1/2} \approx 1.3R(t\kappa)^{1/2}. \tag{11}$$

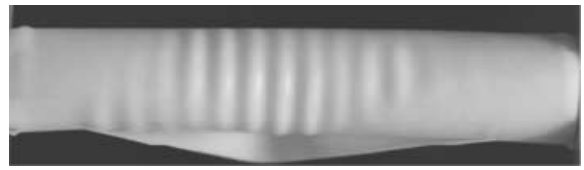

Fig. 2 – When the voluted rubber scroll is compressed axially, a rippling pattern similar to the one in fig. 1 appears. A calculation similar to the one in the text then leads to the following expressions: $\lambda = 2\pi(tR)^{1/2}/\sqrt{3} \approx 3.6(tR)^{1/2}$, $A = \lambda(\kappa R)^{1/2}/\pi^{1/2} \approx 1.46R(t\kappa)^{1/2}$, and yields results in agreement with observations. The small difference in the amplitude from the result for the bent tubes arises from the difference in the strain distribution in the two cases; however, the wavelength remains the same. We note that this configuration is energetically unstable for isolated thin cylindrical shells which prefer to buckle into an almost inextensible surface patterned by diamond-like buckles; here however, the multi-layered structure stabilizes the axisymmetric state.

Although the wavelength we predict is the same as that for the onset of axisymmetric buckling of a cylindrical shell [12], since our theory is nonlinear from the onset, this is fortituous. Furthermore, the classical result of axisymmetric buckling of a thin shell corresponds to a physically unstable situation; thin single-walled cylinders prefer to buckle into a diamond-like pattern instead of the axisymmetric shape because the latter, which involves a lot of stretching, is energetically very expensive [5]. Here, it is the presence of the multiple layers that stabilizes the axisymmetric shapes. Indeed, we can see this by axially compressing the multi-layered scroll, as shown in fig. 2. An even simpler qualitative experiment emphasizes the role of the inner layers: when a single layer of rubber is wrapped around a solid tube which is then bent, we also see the characteristic rippling instability [13].

When the number of walls $n \gg 1$, the inner radius of the tube is much smaller than the outer radius and $R \approx nt$. Substituting this into (10), (11) yields

$$\lambda \approx 3.6n^{1/2}t, \qquad A \approx 1.3nt^{3/2}\kappa^{1/2}. \tag{12}$$

These scaling laws show how one can generate large length scales in terms of small ones in these systems. The validity of (10), (11) is based implicitly on the assumption of a wide separation of the geometric scales which allows us to consider just the leading-order bending, stretching and inextensibility effects. A quick check shows that since $t \ll A \ll \lambda \ll R \ll L$, the requirement is satisfied. Although the above analyses focused on just the outer layer, the inner layers located at a distance r from the neutral axis of the tube should behave in exactly the same way, with $\lambda \sim (rt)^{1/2}$; $A \sim r(t\kappa)^{1/2}$. However, as can be seen in fig. 1(b), there is a reduction in the amplitude and a flattening of the layers towards the neutral axis due to the effects of the small but finite compressibility of the layers, so that the variations in the wavelength are masked.

To verify our predictions, we rolled macroscopic rubber sheets of varying thicknesses into tubes with a negligibly small core and bent the resulting scrolled tubes into arcs of circles of varying curvature κ. Figure 3(a) shows that the millimeter range wavelength of the rippled rubber tubes and the nanometer range wavelength of the rippled nanotubes [1, 14–16] follow (5), *i.e.* the wavelength is determined primarily by geometry, is independent of κ and is essentially independent of the material properties. The inset in fig. 3(a) shows that the ripples in nanotubes are only slightly longer (in a dimensionless sense, following (10)) than the ripples in rubber tubes. This is probably due to the weak short-range interaction between graphite sheets which increases the effective-layer bending stiffness. In fig. 3(b) the measured

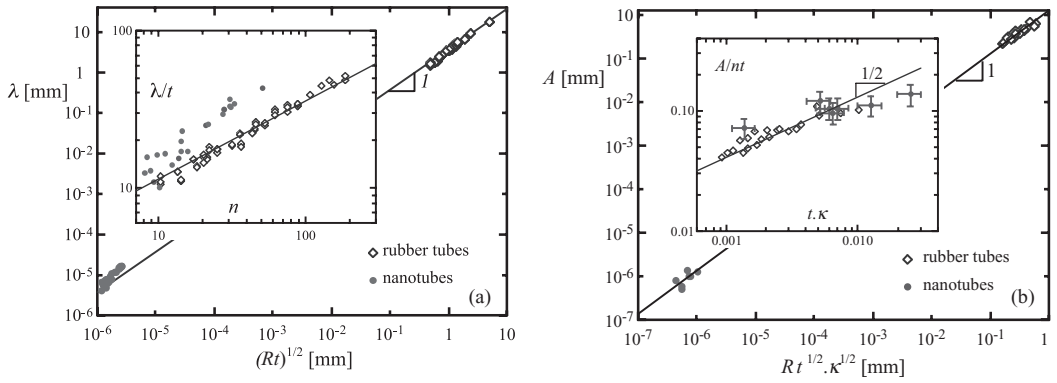

Fig. 3 – Wavelength and amplitude of the rippling patterns. (a) The wavelength of the ripples obeys the predicted scaling law for phenomena separated by six orders of magnitude; the solid line is given by $\lambda = 3.6(tR)^{1/2}$ (10). In the inset the same data is plotted in dimensionless form following (12) and shows that the wavelength of the nanotube ripples is slightly larger than that of the macrotube ripples, consistent with the slight increase in the layer bending stiffness for nanotubes because of a smaller Poisson ratio and the weak interaction between layers. The scatter in the experimental data for small n arises since the tubes sometimes kink via the Brazier buckling mode [3] instead of rippling. (b) The amplitude of the ripples for the macrotubes and the few nanotubes for which this data is available also falls on the theoretical line $A = 1.3R(t\kappa)^{1/2}$ (11). The inset shows the same data plotted in dimensionless form following (12). The nanotube data was obtained from [1, 14–16].

amplitude of the ripples is seen to follow the law (11), confirming the validity of our theory for finite deformations.

Our analysis illuminates the geometric mechanisms which generate mesoscopic length scales from atomic ones, in sharp contrast to the computational [17–20] approaches to these problems using atomistic and continuum ideas which depend on the detailed interactions in each system. Consideration of the microscopic physics reveals differences between the nanotubes and rubber tubes; in the former the attractive short-range van der Waals forces couples the deformations of individual layers, while in the latter the frictional interaction between layers plays a similar role. In particular, this leads to an asymmetry in the crests and the troughs of the ripples, seen in the nano and macro scrolls which arises due to the fact that there is a large but finite compressibility of the multi-layer scroll. However, the primary role of the multi-layered geometry is to induce an effective anisotropy in the system via the steric hindrance that prevents very long-wavelength deformations, but nevertheless allows the layers to slide over each other relatively easily allowing us to treat each single layer separately. This is reminiscent of liquid-crystal systems such as smectics [21], although a crucial difference is the ability of each layer in our purely elastic system to resist shear deformations, something that the individual smectic layers cannot do owing to their in-plane fluid-like behavior. Indeed, the analogy to smectics may be carried further. The competition between bending and layer compression leads to a characteristic length scale of localization that scales as $(Et^2/K)^{1/2}$, where K is the compression modulus of the multi-layer; this describes the crest-trough asymmetry and depends on the short-range repulsive nature of the van der Waals force for nanotubes, and the looseness of the packing for the rubber tubes, although the details of this are best left for another study.

The independence of the rippling pattern on material properties is indicative of the gener-

ality of our theory, which depends on the effective anisotropy of the system generated by the layered structure. Thus, we can expect to see similar patterns in elastomeric liquid-crystalline systems that are solid-like in the plane in such cases as smectic layers, micellar onion phases and layered focal conics. On a completely different scale, we should also expect to see this rippled phase in macroscopic systems such as the kinking of timber [22] which is a layered cylindrical structure, and in geological formations that are often layered. Indeed, our theory might perhaps explain even the wrinkling of an elephant's trunk, suggesting the epithet "Ganesha" instability after the mythical elephant god from India!

* * *

We thank M. Warner for his suggestions on the manuscript. LM thanks the ONR YIP program and the Schlumberger Chair Fund for support. JB and GHM thank the Cambridge-MIT Institute (CMI) program on Carbon Nanotube Enabled Materials for support.

REFERENCES

[1] Poncharal P., Wang Z. L., Ugarte D. and de Heer W. A., *Science*, **283** (1999) 1513.
[2] Although the hexagonal lattice in the nanotubes leads to anisotropic material properties, here we will ignore this, since the lattice is essentially isotropic on scales of a wavelength or longer.
[3] Brazier L. G., *Proc. R. Soc. London, Ser. A*, **116** (1927) 104.
[4] Lobkovsky A. E., *Phys. Rev. E*, **53** (1996) 3750.
[5] Kyriakides S. and Ju G. T., *Int. J. Solids Struct.*, **29** (1992) 1117.
[6] Love A. E. H., *A Treatise on the Mathematical Theory of Elasticity*, 2nd edition (Dover) 1944.
[7] Cerda E. and Mahadevan L., *Phys. Rev. Lett.*, **90** (2003) 074302.
[8] This assumption is asymptotically correct if the wavelength of the ripples is much smaller than the outer radius of the tube. A consistency check later verifies this.
[9] Actually, there is a weak dependence on the Poisson ratio, as we will see later.
[10] The only axial strain arises due to bending, and can thus be written in terms of κ_r. Similarly, the azimuthal variations in strain also arise purely due to radial displacements. All other components of the displacement and strain are sub-dominant. This simplified picture can be justified using an asymptotic expansion in t/R and relies on the presence of disparate multiple length scales in the problem.
[11] Here we impose the inextensibility condition only in an integrated form as an approximation that allows us to circumvent a much more complicated result that accounts properly for the effects of local Poisson contraction.
[12] Timoshenko S. P. and Gere J., *Theory of Elastic Stability*, 2nd edition (McGraw-Hill) 1963.
[13] We thank an anonymous referee for suggesting this.
[14] Falvo M. R. *et al.*, *Nature*, **389** (1997) 582.
[15] Lourie O., Cox D. M. and Wagner H. D., *Phys. Rev. Lett.*, **81** (1998) 1638.
[16] Bower C., Rosen R., Jin L., Han J. and Zhou O., *Appl. Phys. Lett.*, **74** (1999) 3317.
[17] Yakobson B. Y., Brabec C. J. and Bernholc J., *Phys. Rev. Lett.*, **76** (1996) 2511.
[18] Liu J. Z., Zheng Q. and Jiang Q., *Phys. Rev. Lett.*, **86** (2001) 4843.
[19] Qiang D. *et al.*, *Appl. Mech. Rev.*, **55** (2002) 495.
[20] Pantano A., Parks D. M. and Boyce M. C., preprint (2003).
[21] de Gennes P. G. and Prost J., *Physics of Liquid Crystals*, 2nd edition (Oxford) 1993.
[22] Gordon J. E., *Structures* (Penguin) 1991, Chapt. 13.